NASA TECHNICAL NOTE

NASA TN D-5506

c. 1

TECH LIBRARY KAFB, NM
0132130

NASA TN D-5506

LOAN COPY: RETURN TO
AFWL (WLOL-2)
KIRTLAND AFB, N MEX

EFFECTS OF THREE OUTLET-ANNULUS AREA BLOCKAGE CONFIGURATIONS ON THE PERFORMANCE OF A 20-INCH (50.8-CM) AXIAL-FLOW COMPRESSOR ROTOR

by Walter M. Osborn and George W. Lewis, Jr.

Lewis Research Center
Cleveland, Ohio

NATIONAL AERONAUTICS AND SPACE ADMINISTRATION • WASHINGTON, D. C. • OCTOBER 1969

TECH LIBRARY KAFB, NM

0132130

1. Report No. NASA TN D-5506	2. Government Accession No.	3. Recipient's Catalog No.
4. Title and Subtitle EFFECTS OF THREE OUTLET-ANNULUS AREA BLOCKAGE CONFIGURATIONS ON THE PERFORMANCE OF A 20-INCH(50.8-CM) AXIAL-FLOW COMPRESSOR ROTOR		5. Report Date October 1969 6. Performing Organization Code
7. Author(s) Walter M. Osborn and George W. Lewis, Jr.		8. Performing Organization Report No. E-4783
9. Performing Organization Name and Address Lewis Research Center National Aeronautics and Space Administration Cleveland, Ohio 44135		10. Work Unit No. 720-03 11. Contract or Grant No.
12. Sponsoring Agency Name and Address National Aeronautics and Space Administration Washington, D.C. 20546		13. Type of Report and Period Covered Technical Note 14. Sponsoring Agency Code

15. Supplementary Notes

16. Abstract

An inlet-stage axial-flow rotor was tested with tip annulus flow blockages of 22, 55, and 75 percent inserted downstream of the rotor. All three blockages eliminated rotating stall at speeds as high as 0.7 of design and enabled the rotor to be operated under stable conditions to much lower flows than that of the unblocked rotor. Torque values of 83, 64, and 52 percent of the unblocked rotor resulted from blocking 22, 55, and 75 percent of the air flow, respectively, at 0.7 of design speed. The rotor efficiency was adversely affected by the blockages with losses of 22, 38, and 44 percentage points, respectively, at 0.7 of design speed. Blade temperatures and stresses remained within operational limits.

17. Key Words *(Suggested by Author(s))* Compressors Flow blockage Torque reduction Rotating stall	18. Distribution Statement Unclassified - unlimited

19. Security Classif. (of this report)	20. Security Classif. (of this page)	21. No. of Pages	22. Price *
Unclassified	Unclassified	24	$3.00

*For sale by the Clearinghouse for Federal Scientific and Technical Information
Springfield, Virginia 22151

EFFECTS OF THREE OUTLET-ANNULUS AREA BLOCKAGE CONFIGURATIONS ON THE PERFORMANCE OF A 20-INCH (50.8-CM) AXIAL-FLOW COMPRESSOR ROTOR

by Walter M. Osborn and George W. Lewis, Jr.

Lewis Research Center

SUMMARY

An inlet-stage axial-flow rotor was tested with tip annulus flow blockages of 22, 55, and 75 percent inserted downstream of the rotor. In all three cases, the blockage eliminated rotating stall at speeds as high as 0.7 of design and enabled the rotor to be operated under stable conditions to much lower flows than that of the unblocked rotor.

At 0.7 of design speed, torque values of 83, 64, and 52 percent of the unblocked rotor resulted from blocking 22, 55, and 75 percent of the air flow, respectively. At 0.4 of design speed, the corresponding torque values were 108, 73, and 68 percent of the unblocked rotor. The torque reductions resulting from 55 and 75 percent flow blockage might be of sufficient magnitude to enable a low-cost starting system to be considered for some turbofan-type engines. At speeds greater than 0.5 of design, all three flow blockages might be useful for reducing engine thrust for aircraft maneuvers where low thrust and high engine rpm are desirable. Flow blockage might also be of use for improving engine acceleration characteristics of some engines.

The rotor efficiency was adversely affected by the insertion of flow blockage. At 0.7 of design speed, the losses in efficiency resulting from blocking 22, 55, and 75 percent of the air flow were approximately 22, 38, and 44 percentage points, respectively.

All three blockages resulted in higher temperatures just upstream of the rotor than that in the upstream plenum chamber. The temperature generally increased from the hub to the blade tip. The maximum temperature observed was 734° R (408 K) with 55 percent flow blockage. However, for the 75 percent flow blockage, the temperature was increasing with time, and the equilibrium temperature for this case would probably exceed the value of 734° R (408 K). Thus, in an operating engine using high flow blockages, temperature monitors might be desirable.

The maximum vibratory blade stresses (compression and tensile) for the 22, 55,

and 75 percent flow blockage configurations were ±1200 psi (8.26×10^6 N/m^2), ±3000 psi (20.65×10^6 N/m^2), and ±3000 psi (20.65×10^6 N/m^2), respectively. These low stress levels indicate an absence of rotating stall that was substantiated by inlet surveys with a hot-wire anemometer probe.

INTRODUCTION

Several operational conditions for jet engines make desirable the partial blockage of the air flow passage either upstream or downstream of the compressor. Air flow blockage devices may be utilized to improve the compressor operational stability at off-design speeds, reduce the compressor starting torque requirements, reduce engine thrust for some maneuvers, and possibly improve engine acceleration characteristics in engines where this would be desirable. Such devices would be particularly adaptable to the turbofan engine because of the division of the inlet air into by-pass air and gas generator (core engine) air. Thus, the by-pass air could be blocked downstream of the fan rotor to obtain the aforementioned benefits.

Some experience has been obtained with flow blockage devices for turbojet engines with conventional axial-flow compressors. For these compressors, flow blockage was placed upstream of the inlet guide vanes. The aims of these tests were to improve the match between the inlet and outlet stages of the axial-flow compressor at off-design speeds, suppress rotating stall in the inlet-stage rotor, and reduce the first-stage rotor blade vibrational stress. Without blockage and at low or intermediate compressor speeds, some of the inlet stages of the compressor may be operating with a rotating stall condition because the design ratio of compressor inlet to discharge annulus area is too large at low speeds. If too many of the inlet stages are stalled, premature compressor surge may be triggered, which reduces the margin between the compressor equilibrium operating line required for normal engine operation and the compressor surge line. During transient conditions such as engine acceleration, the compressor operating condition goes above the equilibrium operating line and approaches the surge line. If the margin between the two lines is small, the maximum allowable rate of engine acceleration is limited. Applying inlet blockage to adjust the inlet to outlet area ratio may suppress rotating stall in the inlet-stage rotor and thus improve the performance of both the compressor and the engine.

In an early NACA investigation of a turbojet engine with a 13-stage axial-flow compressor, inlet baffles at either the hub or tip successfully eliminated rotating stall and reduced vibratory stress measured in the inlet-stage rotor blades by a factor of 5 (ref. 1). In references 2 and 3, hub baffles suppressed rotating stall and reduced blade stress in a 15-stage axial-flow compressor. However, in the investigation of refer-

ence 2, tip baffles were not effective. Thus, experimental testing appears to be required for each compressor design to determine the effectiveness of various blockage techniques. Although inlet flow blockage was shown to be effective, other methods for improving compressor stage matching at off-design speeds have been used more extensively than flow blockage devices. These methods include adjustable inlet guide vanes, variable stators, compressor discharge bleed, interstage bleed, and two-spool compressors (ref. 4).

In the turbofan engine with its division of the inlet air flow into by-pass air and core engine air, flow blockage can be used for applications other than that of improving the match between inlet and outlet stages of the compressor. Tip annulus blockage downstream of the fan can be used as a device to block the fan rotor by-pass air to reduce the power absorbed by the fan during engine startup. Also, various degrees of blockage of the by-pass air can provide variable thrust control while high engine speed is maintained. For a downstream flow blockage device to be successful, however, it must suppress rotating stall in the fan rotor as did the upstream flow blockage devices in the investigations of references 1 to 3.

The purpose of this investigation was to determine the effectiveness of downstream tip annulus blockage in the suppression of rotating stall and in the improvement of the operational stability of a simulated fan rotor at off-design speeds. The effectiveness of such a device in reducing the power requirements of the fan rotor during engine startup was also part of the study. The rotor used in the investigation is for a modern axial-flow inlet stage having high pressure rise and high relative Mach number. Three separate downstream tip annulus blockage configurations were used with the rotor to simulate turbofan engines with different by-pass air ratios or different size core engines.

Blocking the air flow downstream of the rotor results in an induced eddy circulation in and ahead of the blocked portion of the rotor. Such a circulation could possibly increase the temperature of the rotor blades beyond safe operational limits. An examination of this temperature rise was also part of this investigation.

SYMBOLS

N_D design speed, 16 000 rpm

W actual air weight flow, lbm/sec; kg/sec

δ ratio of inlet (plenum) total pressure to NACA standard sea-level pressure of 29.92 in. Hg abs (10.10×10^4 N/m^2 abs)

η_{ad} adiabatic temperature-rise efficiency

θ ratio of inlet (plenum) total temperature to NACA standard sea-level temperature of 518.69° R (288.16 K)

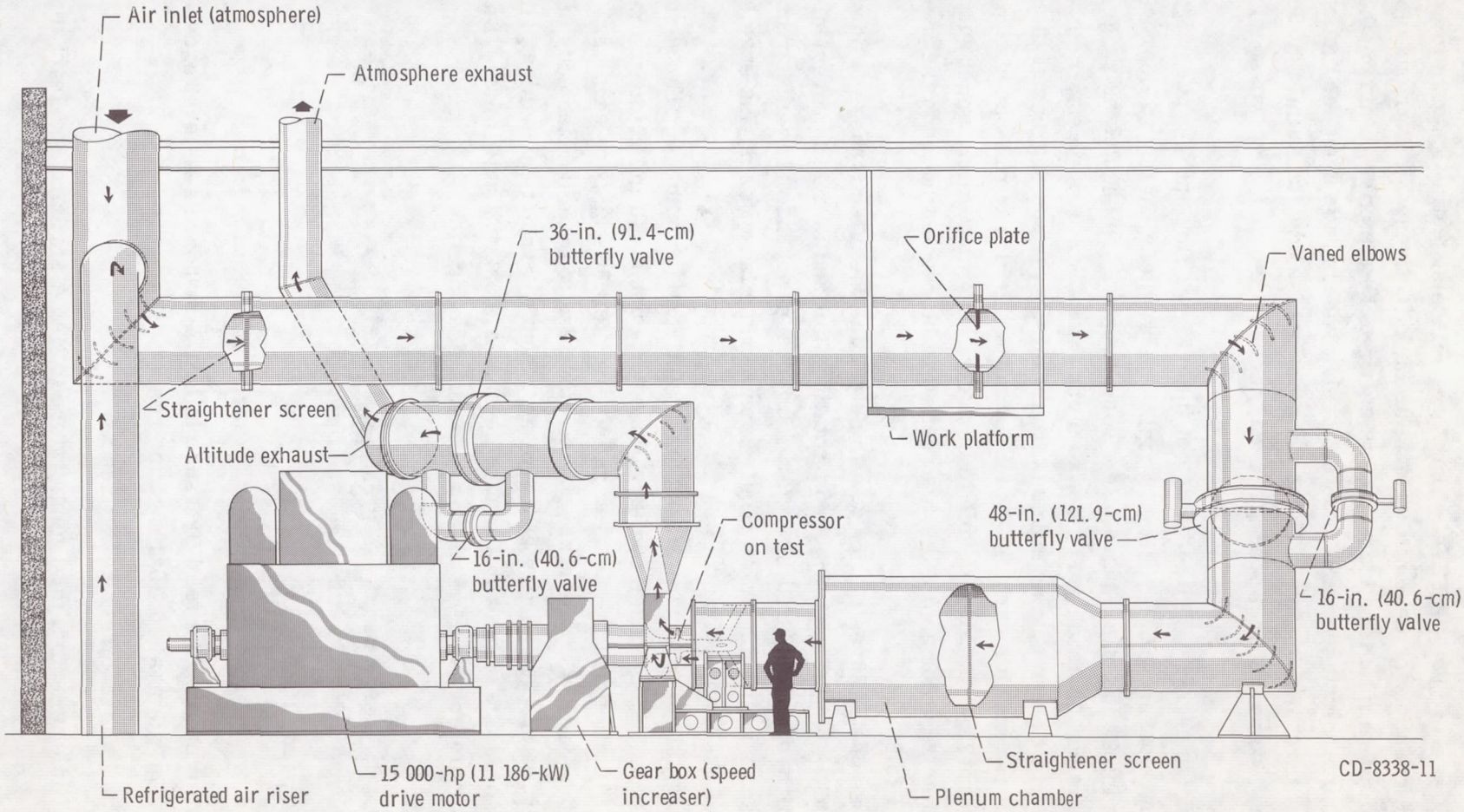

Figure 1. - Test facility.

APPARATUS

Test Facility

A schematic diagram of the test facility is shown in figure 1. The drive system consists of a 15 000-horsepower (11 186-kW) electric motor with a variable-frequency speed control. The motor was coupled to a 5.02-ratio speed-increaser gearbox that drove the test rotor. The air supply was atmospheric air. The facility was operated with altitude exhaust at 26 inches of mercury absolute (8.8×10^4 N/m^2 abs) downstream of the test rotor. Air flow was controlled by butterfly valves in the inlet and outlet lines. Air flow was measured by a thin-plate orifice, 27.2 inches (69.1 cm) in diameter, located in the 48-inch (121.9-cm) inlet line. A plenum tank 6 feet (1.83 m) in diameter and approximately 12 feet (3.66 m) long was located just upstream of the test rotor. A bellmouth nozzle was fitted from the plenum tank to the inlet of the test rotor.

Instrumentation

Two bare-wire thermocouples were located at the center of the plenum tank for sensing inlet total temperature. Inlet plenum total pressure was determined from two manifolded wall static taps located 90° apart on the plenum tank. A shielded total pressure probe was placed downstream of the test rotor at midpassage height for monitoring the rotor outlet pressure and setting the test operating points. The rotor outlet conditions were determined by two radial traversing combination sensing probes located 1 inch (2.54 cm) downstream from the blade tip trailing edge and 90° apart circumferentially. Radial distribution of total temperature, total pressure, and flow angle were obtained from the combination probes. Static pressure was determined by radial surveys made with two 18° static wedge pressure probes. Radial surveys were made with a combination probe located 1 inch (2.54 cm) upstream of the blade tip leading edge at one circumferential location. A radial traversing hot-wire anemometer probe also located 1 inch (2.54 cm) upstream of the rotor was used for monitoring the inlet flow conditions and detecting the presence of rotating stall. The combination sensing probe is shown in figure 2, and its operation is described in reference 5.

Rotor and Blockage Configurations

The rotor used in this investigation had a nominal diameter of 20 inches (50.8 cm) and 47 blades. The hub-tip radius ratio at the inlet was 0.5. The rotor was equipped

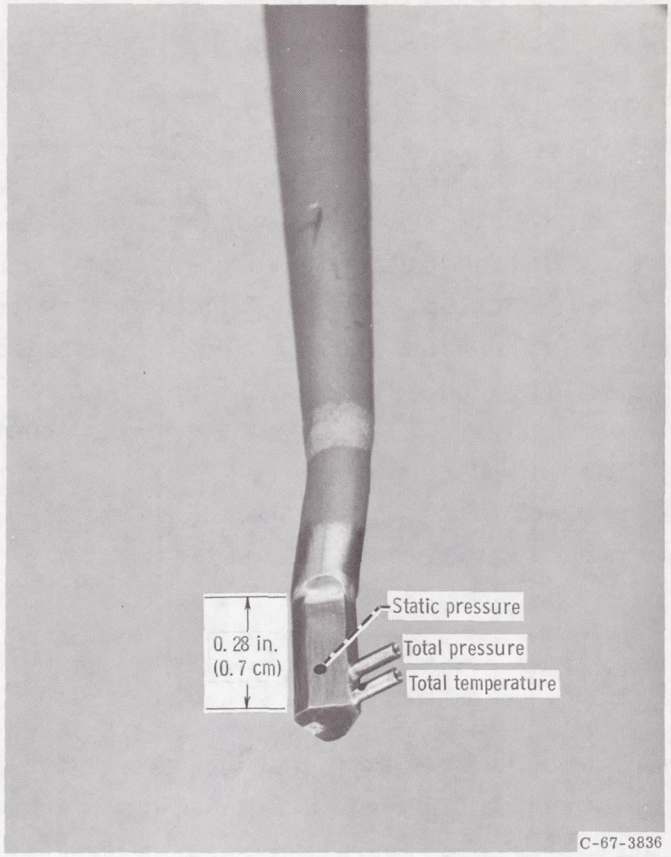

Figure 2. - Combination sensing probe.

with blade vibration dampers, and 10 blades were instrumented with strain gages to monitor the blade stress during the investigation. The rotor (fig. 3) was designed for the first stage of a high-pressure-ratio axial-flow compressor and had a design diffusion factor of 0.45. Design operating speed N_D was 16 000 rpm or an inlet tip speed of about 1396 feet per second (426 m/sec).

Meridional plane profiles of the rotor, shrouding, and three blockage configurations considered are shown in figure 4. The unblocked theoretical design streamline nearest the inner surface of each block was used to assign nominal flow blockage values of 22, 55, and 75 percent to the three configurations. The actual annular area blockages at the upstream edge of the annular block corresponding to the nominal values are 23.9, 55.7, and 74.2 percent, respectively. The inner surface of the 75 percent flow block was contoured to match the unblocked design flow streamline. The inner surface of the other two blockage configurations were constant radii since their unblocked design flow streamlines were nearly parallel to the axis of rotation. Also shown in figure 4 are the locations of the inlet and outlet radial survey instrumentation planes.

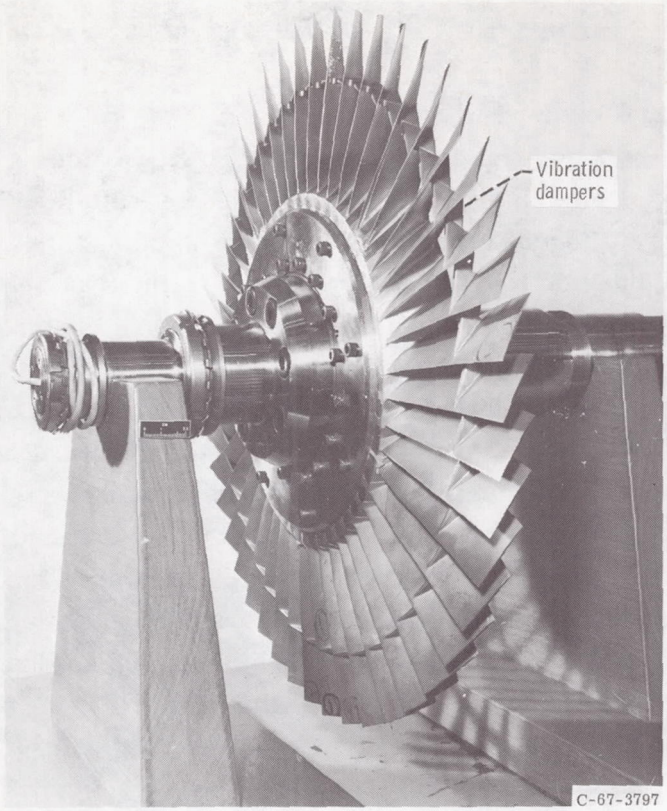

Figure 3. - 20-Inch (50.8-cm) axial-flow compressor rotor.

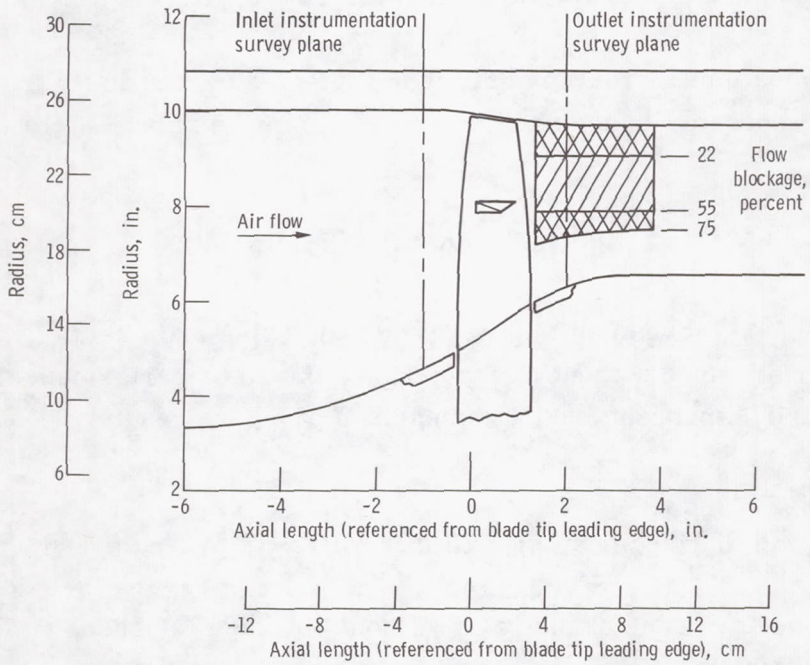

Figure 4. - Meridional view of axial-flow rotor showing three blockage configurations.

PROCEDURE

The tests were conducted using atmospheric air at the rotor inlet with the inlet control valve in the fully open position throughout the tests. Altitude exhaust was used at the rotor outlet to help overcome the losses in the discharge system. The unblocked rotor was tested over a range of speeds from 0.4 of design to design. The flow was varied from choke flow (fully open outlet flow control valve) to the flow at which audible surge occurred except at design speed. At design speed, the surge point was not obtained to prevent possible damage to the rotor. At speeds of 0.4 to 0.7 of design, the rotor performance at flow rates lower than the surge point flow rate was also investigated.

The blocked rotor was tested over a range of speeds from 0.2 to 0.7 of design. The flow range was obtained by changing the outlet flow control valve setting from the fully open to the fully closed position. Air leakage through the closed outlet flow control valve determined the minimum flow point for each performance curve for the blocked rotor.

The overall rotor performance is based on average conditions in the depression or plenum tank and mass-averaged values of temperature and pressure at the rotor outlet as determined by outlet radial surveys taken approximately 1 inch (2.54 cm) downstream from the blade tip trailing edge (fig. 4). Inlet radial surveys of temperature were taken 1 inch (2.54 cm) upstream of the blade tip leading edge (fig. 4). All performance parameters were based on plenum measurements corrected to standard sea-level conditions. The rotor torque was calculated from the temperature ratio (ratio of absolute values of outlet total temperature to plenum total temperature), equivalent weight flow, and rotor speed.

The flow fluctuations of rotating stall were detected by a radially traversing hot-wire anemometer probe located 1 inch (2.54 cm) upstream of the blade tip leading edge (fig. 4).

RESULTS AND DISCUSSION

The results of this investigation are presented in five main sections. These constitute the rotor performance without flow blockage, the rotor performance with flow blockages of 22, 55, and 75 percent, and a comparison of all the results.

Rotor Performance Without Annulus Area Blockage

The overall performance of the rotor without blockage is presented in figure 5 as curves of pressure ratio, efficiency, and torque as a function of equivalent weight flow for various fractions of design speed from 0.4 to 1.0. At design speed, a maximum rotor

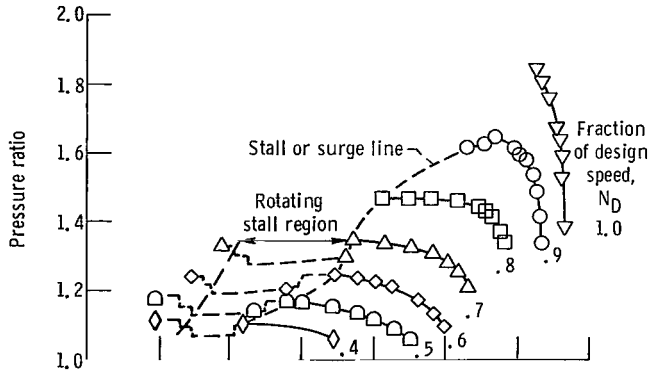

(a) Pressure ratio as function of weight flow.

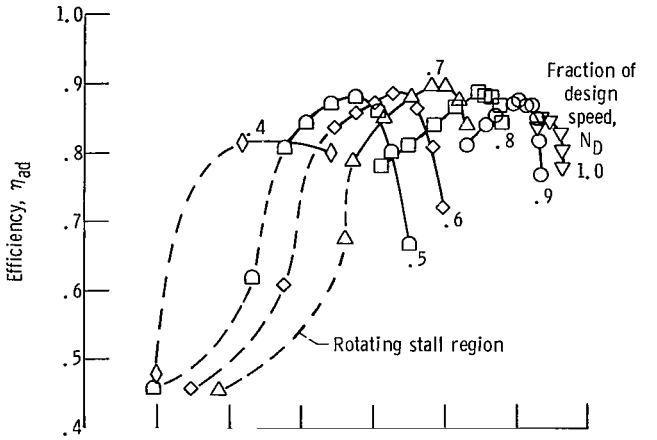

(b) Efficiency as function of weight flow.

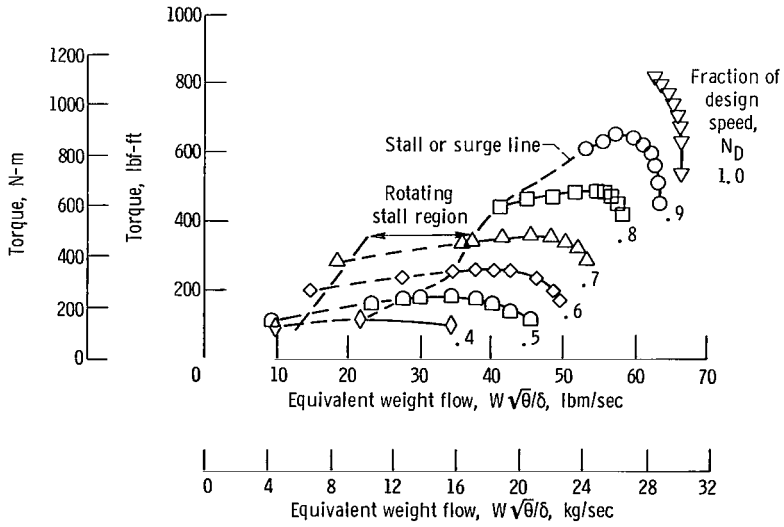

(c) Torque as function of weight flow.

Figure 5. - Rotor performance without blockage.

efficiency of 0.846 was obtained at a pressure ratio of 1.80 and an equivalent weight flow of 63.50 pounds per second (28.8 kg/sec).

The stall limit line (fig. 5(a)) was determined by the use of a hot-wire anemometer to indicate the presence of rotating stall at the inlet to the rotor. With this rotor, audible surge and rotating stall occurred at approximately the same time. At design speed, the stall limit point was not determined in order to avoid high blade stress due to violent stall or surge.

Rotor performance in the rotating stall region to the left of the stall line (figs. 5(a) and (c)) was explored at the lower speeds, 0.4 to 0.7 of design. The performance for the rotor in this area is shown by the dashed lines in figure 5. Only a few data points were taken in the rotating stall region, and the dashed performance curves of figure 5(a) were constructed from the operational monitoring charts. The inlet annulus flow was continuously monitored by a hot-wire anemometer probe, and rotating stall existed over the dashed portions of the performance curve. At the lowest weight flow points (end points) for all the performance curves at rotating speeds from 0.4 to 0.7 N_D, rotating stall disappeared. Efficiencies dropped off rapidly in the rotating stall region and were quite low at the lowest weight flow points ($\approx$0.46 for 0.4 to 0.7 of design speed).

In the rotating stall region, the maximum vibratory blade stress as sensed by strain gages was approximately $\pm$2500 psi (17.23×10^6 N/m^2) at 0.7 of design speed. This stress level was well below the operational limit for the rotor. However, operation in the stalled regions at speeds above 0.7 N_D was not attempted to avoid high blade stress and resulting rotor damage.

Rotor Performance With 22 Percent Air Flow Blockage

The performance curves for the 22 percent flow blockage configuration are presented in figure 6 as curves of pressure ratio, efficiency, torque, and temperature ratio as a function of equivalent weight flow for speeds from 0.3 to 0.7 of design. The minimum flow points shown for the various performance curves (fig. 6) do not represent a stall limit or the minimum flow operating point for the blocked rotor but are the minimum obtainable because of air leakage through the closed outlet flow control valve. No evidence of rotating stall was detected by hot-wire anomometer surveys at the inlet to the rotor over the entire outlet flow control valve range from fully open to fully closed and for the speeds investigated. In general, the performance parameters are degraded from those of the unblocked rotor. However, the rotor with exit flow blockage is shown to operate in a stable condition to much lower flow rates than those of the unblocked rotor.

The maximum efficiencies are between 0.67 and 0.72 for the speeds investigated, with the highest efficiency occurring at 0.5 of design speed. The maximum efficiency at a speed of 0.4 of design was estimated because of the wide spacing of the data points, and

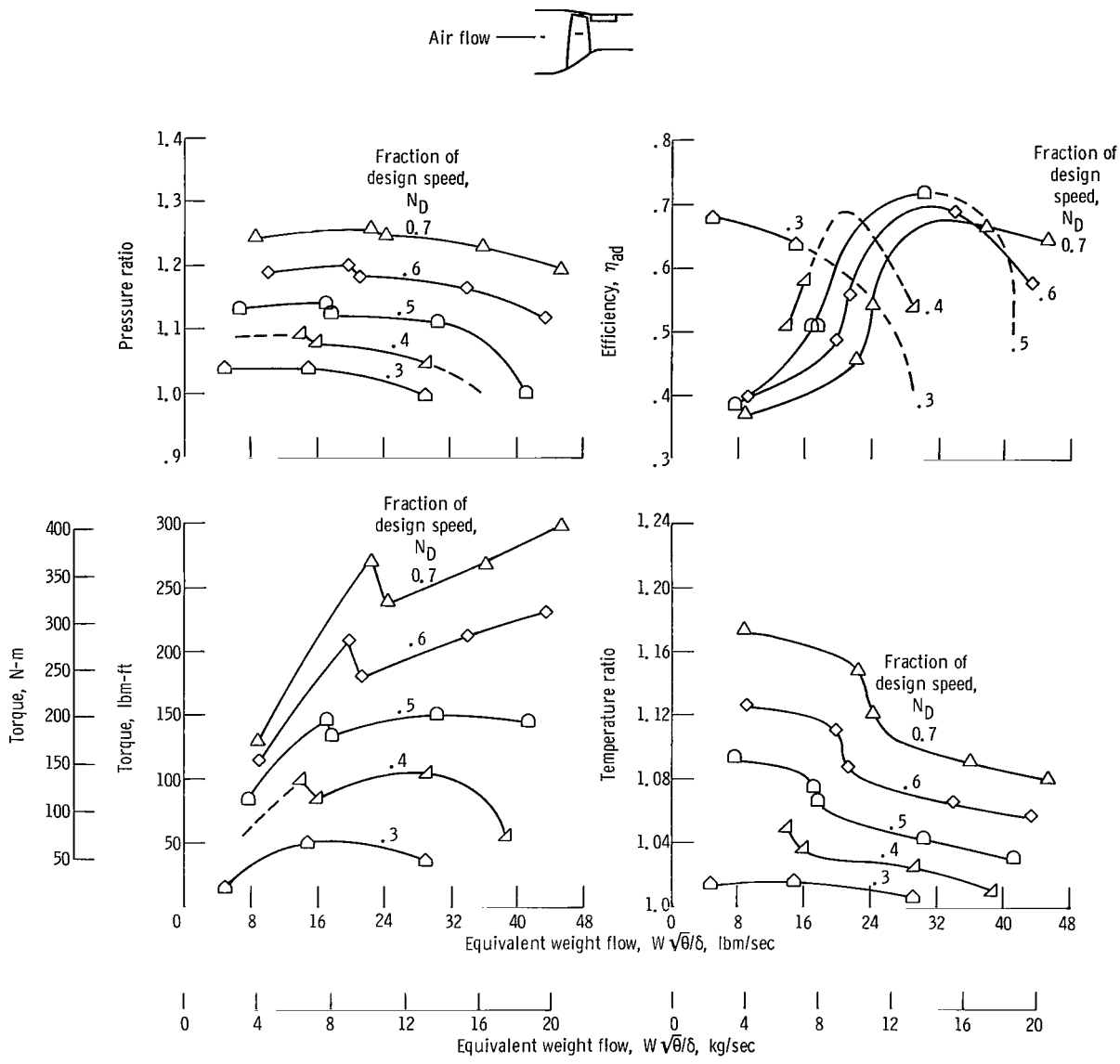

Figure 6. - Rotor performance with 22 percent flow blockage. Rotor diameter, 20 inches (50.8 cm); design speed, 16 000 rpm.

the performance curve is shown as a dashed line in this area. At the maximum flow points for 0.3 and 0.5 of design speed, the efficiencies were very low or could not be calculated because of the low pressure ratio. The performance curves are shown as dashed lines in the maximum flow regions for these speeds.

The performance curves for pressure ratio, torque, and temperature ratio (fig. 6) for speeds of 0.4 to 0.7 of design indicate a slight discontinuity in the curve, wherein all three performance parameters increase rapidly for a small change in weight flow. This discontinuity was more evident in the monitoring chart performance curves, which were

based on outlet midstream instrumentation, than it is in the mass-averaged data presented in figure 6. The discontinuity is thought to be associated with a change in the type of circulation in the eddy flow that is believed to exist in and ahead of the blocked portion of the rotor. The performance curves were repeatable and were generated by slowly closing the outlet flow control valve from the fully open position. However, some effect of hysteresis was noted in the discontinuity portion of the curve as the curve was generated by opening the outlet flow control valve from the fully closed position.

Inlet temperature profiles for 0.5 and 0.7 of design speed are shown in figures 7(a) and (b), respectively, for the minimum flow rate points (highest temperatures). These temperature profiles were obtained from radial surveys of temperature approximately 1 inch (2.54 cm) upstream of the blade tip leading edge. Blocking the flow downstream of the rotor probably results in an induced eddy circulation in and ahead of the blocked por-

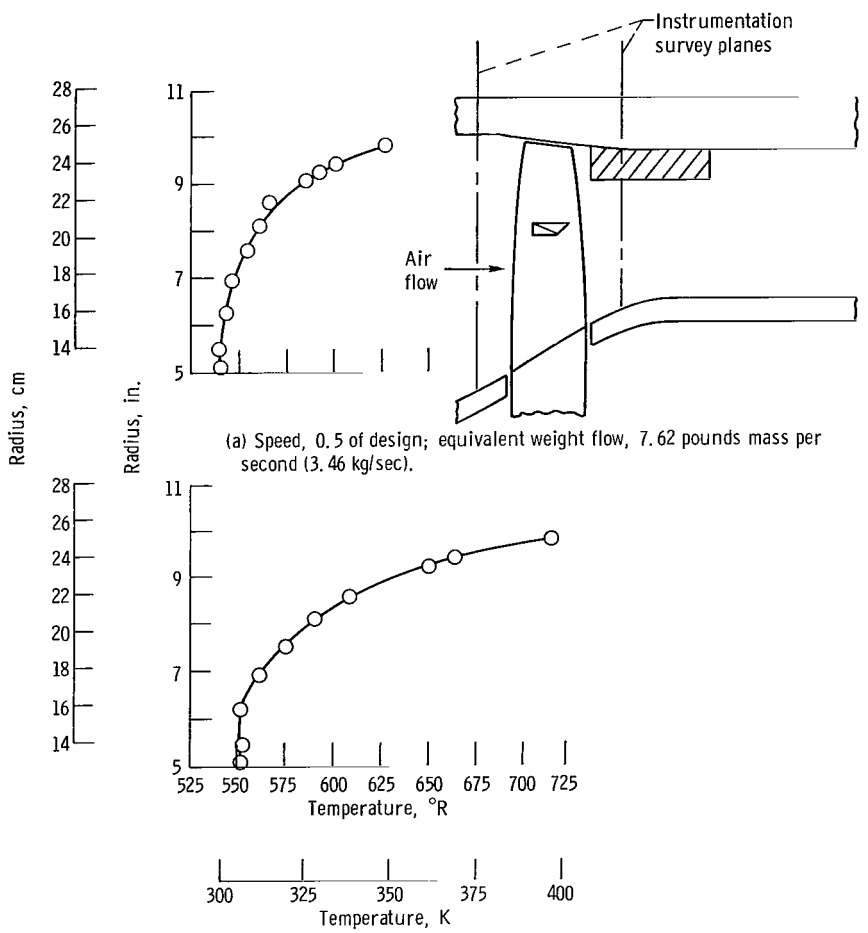

(a) Speed, 0.5 of design; equivalent weight flow, 7.62 pounds mass per second (3.46 kg/sec).

(b) Speed, 0.7 of design; equivalent weight flow, 8.66 pounds per second (3.93 kg/sec).

Figure 7. - Inlet temperature profile for rotor with 22 percent flow blockage. Plenum temperature corrected to standard sea-level condition, 518.69° R (288.16 K).

tion of the rotor. The increase in inlet temperature with increasing radius is apparently caused by the losses in the recirculation or eddy flow that is present. Even the lower temperatures near the hub are considerably higher than the plenum temperature, which indicates a considerable amount of upstream mixing between the eddy circulation and the mainstream flow. For the unblocked rotor, the inlet temperature was nearly constant with radius and essentially the same as plenum temperature, except when the rotor was operating in the unstable or rotating stall region (figs. 5(a) and (c)); in this case, the radial temperature profiles were similar to those of the blocked rotor.

A maximum inlet temperature of approximately 717° R (398 K) was observed near the blade tip for 0.7 of design speed (fig. 7(b)). The maximum temperature did not appear to increase with time, and the rotor was not overstressed at this condition. Apparently, mixing of the eddy flow and main flow was sufficient to stabilize the temperature for any particular operating condition.

Radial surveys of outlet temperature for the blocked rotor showed an increase of only 7.5° R (4.17 K) from the hub to the inner radius of the blockage for both 0.5 and 0.7 of design speed.

The maximum vibratory blade stress measured with the strain gages on 10 blades was approximately ±1200 psi (8.26×10^{6} N/m^{2}) for the rotor with 22 percent flow blockage. This low stress level indicates an absence of rotating stall, which was substantiated by the hot-wire anemometer surveys at the rotor inlet.

Rotor Performance With 55 Percent Flow Blockage

The 55 percent flow blockage configuration had the inner contour of the blockage in line with the blade vibration dampers shown in figure 3. The performance curves for the 55 percent flow blockage configuration are presented in figure 8 as curves of pressure ratio, efficiency, torque, and temperature ratio as a function of equivalent weight flow for various fractions of design speed from 0.2 to 0.7. The minimum flow points shown for the various performance curves do not represent a stall limit but were the lowest obtainable because of air leakage through the outlet flow control valve. No evidence of rotating stall was detected by hot-wire anemometer surveys at the rotor inlet over the entire outlet flow control valve range from fully open to fully closed and for the speeds investigated.

The maximum efficiencies were between 0.49 and 0.55 for the speed range 0.2 to 0.7 of design. Because of the scatter in the data at 0.2 of design speed, the efficiency curve is estimated and shown as a dashed line. The efficiencies are lower than those of the 22 percent flow blockage configuration and are considerably lower than those of the unblocked rotor. However, similar to the 22 percent flow blockage configuration, it was possible to operate the 55 percent flow blockage configuration in a stable condition to

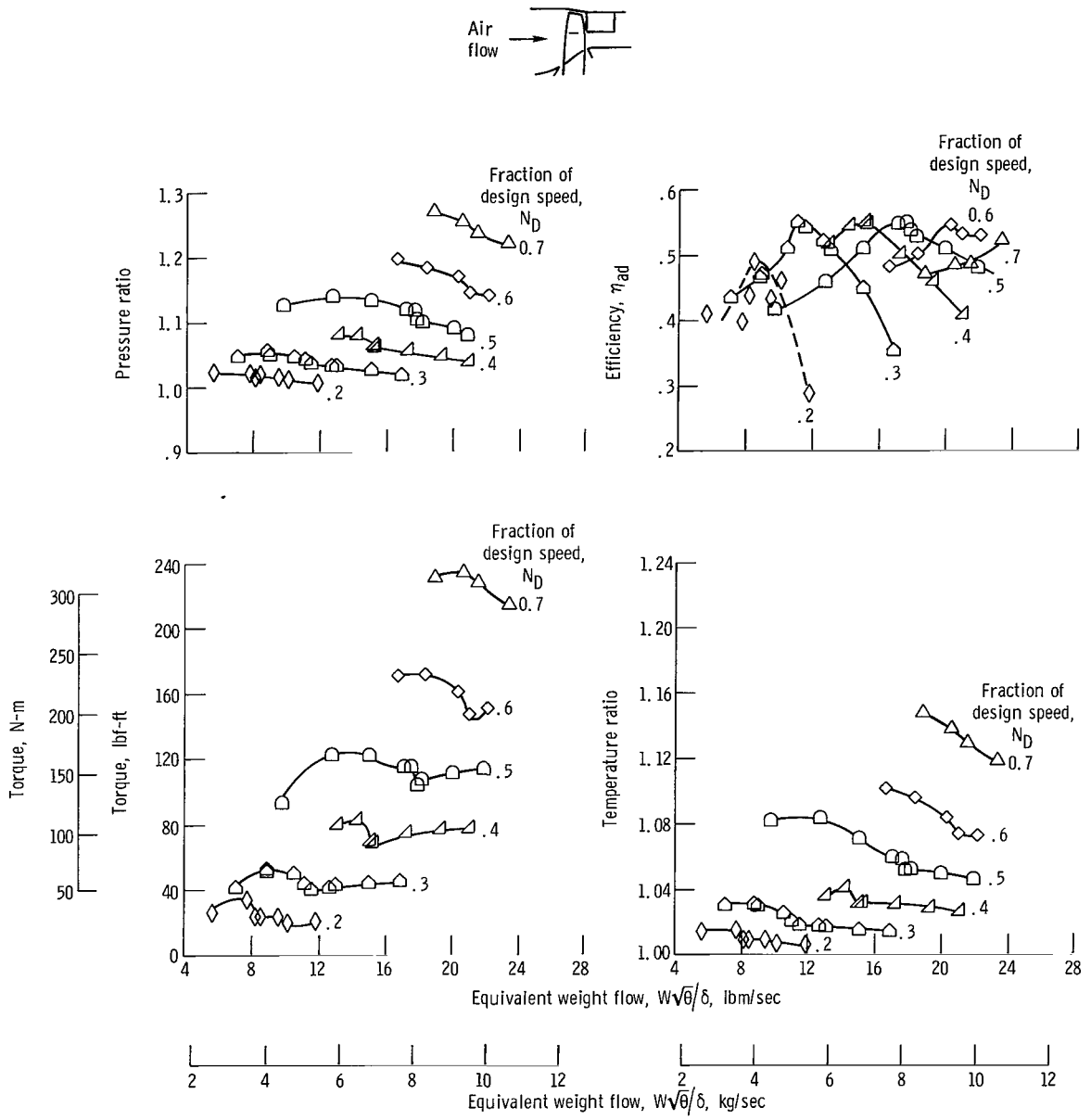

Figure 8. - Rotor performance with 55 percent flow blockage. Rotor diameter, 20 inches (50.8 cm); design speed, 16 000 rpm.

much lower flow rates than those in the case of the unblocked rotor.

The performance curves for pressure ratio, torque, and temperature ratio (fig. 8) exhibited a slight discontinuity at most speeds, as did the performance curves for the 22 percent flow blockage configuration. This discontinuity is believed to be associated with changes in the circulation pattern in the eddy flow in and ahead of the blocked portion of the rotor.

Inlet temperature profiles for 0.5 and 0.7 of design speed are shown in figure 9 for the minimum flow rate points (highest temperatures). At 0.5 of design speed (fig. 9(a)), the inlet temperature increases slowly from 535° R (297 K) near the hub to 545° R (303 K) near the inner radius of the blockage and then increases quite rapidly to 614° R (341 K) near the blade tip. At 0.7 of design speed (fig. 9(b)), the inlet temperature in-

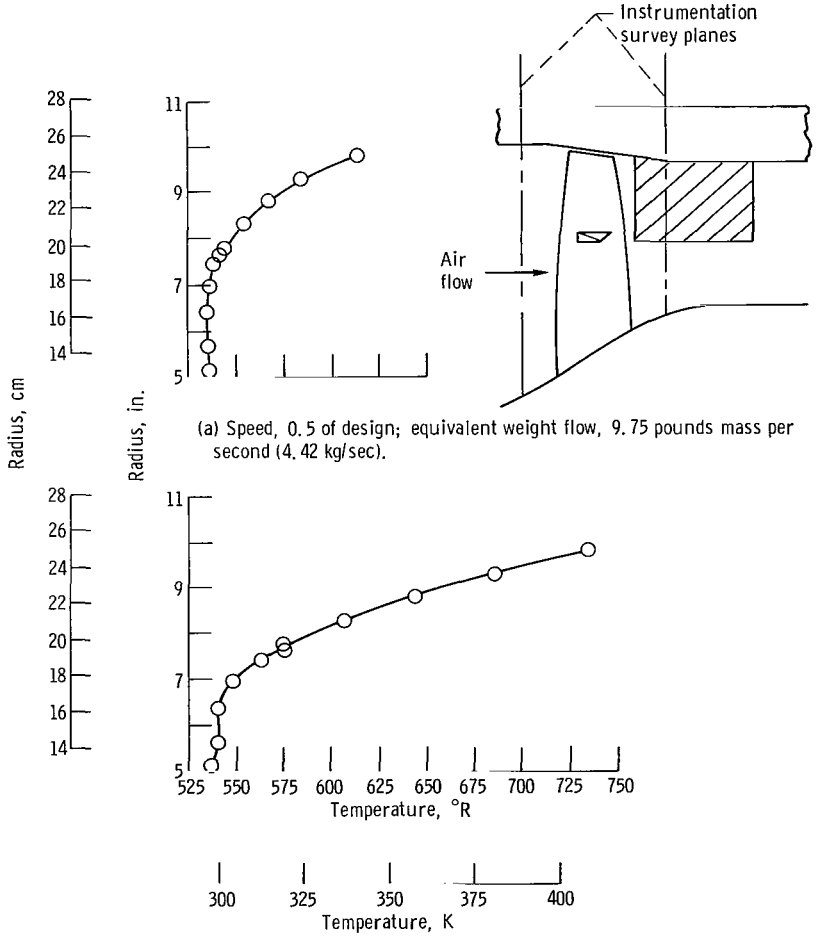

(a) Speed, 0.5 of design; equivalent weight flow, 9.75 pounds mass per second (4.42 kg/sec).

(b) Speed, 0.7 of design; equivalent weight flow, 18.85 pounds mass per second (8.66 kg/sec).

Figure 9. - Inlet temperature profile for rotor with 55 percent flow blockage blockage. Plenum temperature corrected to standard sea-level condition, 518.69° R (288.16 K).

creases at a faster rate, 537° R (298 K) to 574° R (319 K), from near the hub to near the inner radius of the blockage than it did for 0.5 of design speed. The temperature then increases rapidly to 734° R (408 K) near the blade tip. For both 0.5 and 0.7 of design speed, the inlet temperature was considerably higher than the plenum temperature. These temperature profiles indicate an eddy circulation in and ahead of the blocked portion of the rotor and considerable mixing between the eddy circulation and the mainstream flow. The maximum inlet temperature (734° R or 408 K) near the blade tip for 0.7 of design speed (fig. 9(b)) did not increase with time, and the rotor was not overstressed at this condition.

Radial surveys of outlet temperature for the blocked rotor showed a temperature difference of 7.5° R (4.16 K) from near the hub to near the inner radius of the blockage for 0.5 of design speed. At 0.7 of design speed, the outlet temperature difference was 32° R (17.8 K).

The maximum vibratory blade stress was approximately ±3000 psi (20.65×10^6 N/m^2) when the rotor was tested with the 55 percent flow blockage. This low stress level indicates an absence of rotating stall that was substantiated by the hot-wire anemometer surveys at the rotor inlet.

Rotor Performance With 75 Percent Flow Blockage

The performance curves for the 75 percent flow blockage configuration are presented in figure 10 as curves of pressure ratio, efficiency, torque, and temperature ratio as a function of equivalent weight flow for speeds from 0.2 to 0.7 of design. As with the two previous blockage configurations, the minimum flow points shown in figure 10 are the result of a facility limitation. No evidence of rotating stall was detected over either the flow or the speed range. No discontinuities were observed in the performance curves such as were seen in the performance curves for the 22 and 55 percent flow blockage configurations.

The maximum efficiencies for the speeds investigated (fig. 10) are between 0.38 and 0.47 and are nearly constant at 0.47 for the speed range 0.4 to 0.6 of design. These low efficiencies indicate large losses resulting from the recirculating eddy and its intermixing with the main flow stream. Although the efficiencies were much lower than those of the unblocked rotor, the blocked rotor was able to operate in a stable condition to much lower flow rates than could the unblocked rotor.

Inlet temperature profiles for the 75 percent flow blockage configuration at 0.5 and 0.7 of design speeds are presented in figure 11. The curve in figure 11(a) for the minimum flow point at 0.5 of design speed shows an inlet temperature of approximately 547° R (304 K), which is nearly constant from the hub to the inner radius of the blockage. The

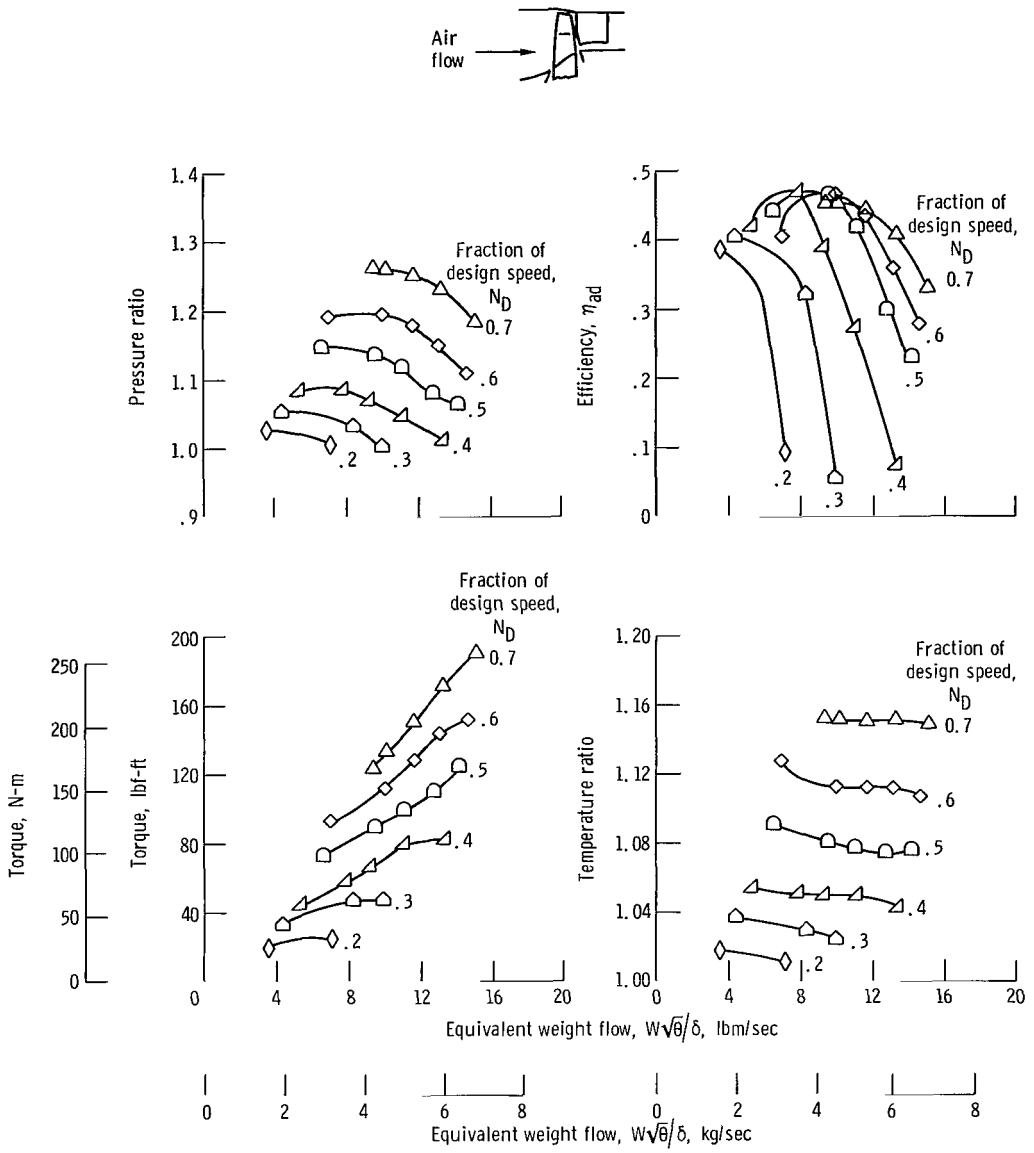

Figure 10. - Rotor performance with 75 percent flow blockage. Rotor diameter, 20 inches (50.8 cm); design speed, 16 000 rpm.

temperature then increases steadily to approximately 621° R (345 K) near the blade tip. Figure 11(b) shows the temperature distribution for 0.7 of design speed at a flow rate of 10.12 pounds mass per second (4.59 kg/sec), which is slightly higher than the minimum flow rate point. The inlet temperature survey data for the minimum flow point appeared to be in error as it did not agree with the temperatures obtained from monitoring thermocouples and also showed a temperature profile different from those obtained for the other blockage configurations. Figure 11(b) shows the inlet temperature steadily increasing from approximately 560° R (311 K) at the inner radius of the blockage to approximately

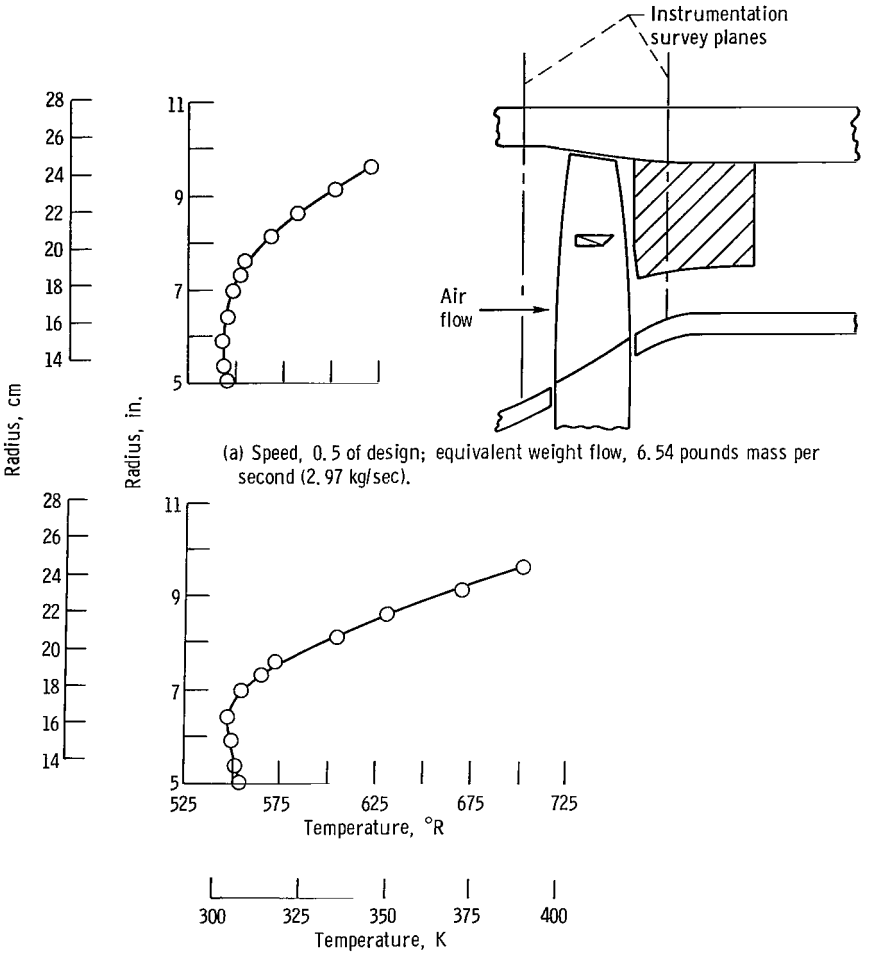

(a) Speed, 0.5 of design; equivalent weight flow, 6.54 pounds mass per second (2.97 kg/sec).

(b) Speed, 0.7 of design; equivalent weight flow, 10.12 pounds mass per second (4.59 kg/sec).

Figure 11. - Inlet temperature profile for rotor with 75 percent flow blockage. Plenum temperature corrected to standard sea-level condition, 518.69° R (518.69 K).

701° R (390 K) near the blade tip. Thus, the temperature profile at this flow rate is similar to those observed for the minimum flow points for the other blockage configurations.

At the minimum flow points for 0.5 and 0.7 of design speed, the temperature near the blade tip was observed for approximately 10 minutes after the inlet temperature radial survey data were obtained. For the 22 and 55 percent flow blockage configurations, the temperature was constant during the observation time. For the 75 percent flow blockage configuration, the temperature increased approximately 25° R (14 K) during the observation period, and it is possible that an equilibrium temperature might be reached that would be above the operational temperature limit for the rotor. Thus, in an operating engine using high flow blockages, temperature monitors might be desirable.

Radial surveys of outlet temperature for the 75 percent flow blockage configuration indicated a temperature difference from the hub to the inner radius of the blockage of less than 10° R (5.6 K) at the minimum flow rate point for both 0.5 and 0.7 of design speed. At 0.7 of design speed and a flow rate slightly greater than the minimum, the difference was approximately 17° R (9.4 K).

Maximum blade vibratory stress was approximately ±3000 psi (20.65×10^6 N/m^2) for the 75 percent flow blockage configuration. This low stress level indicates an absence of rotating stall for this configuration and confirms the result of the hot-wire anemometer surveys at the rotor inlet.

Comparison of Unblocked and Blocked Rotor Configurations

A comparison of the maximum efficiencies for the rotor with 22, 55, and 75 percent flow blockages and the unblocked rotor is shown in figure 12. The curve for 22 percent

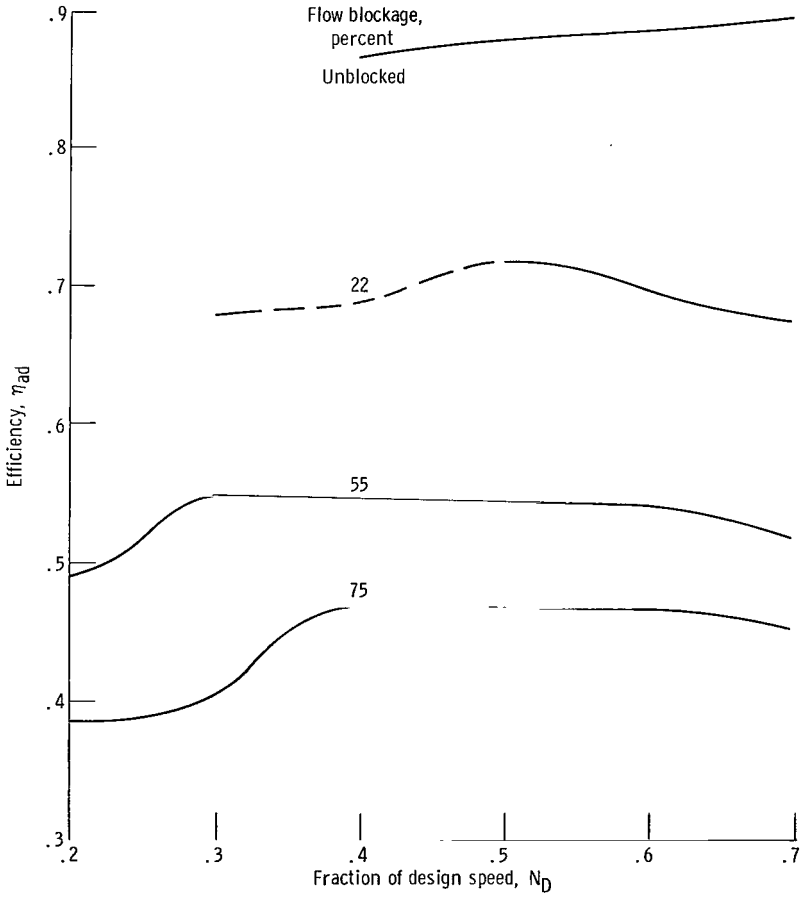

Figure 12. - Comparison of maximum efficiency for unblocked and blocked rotor configurations.

flow blockage is dashed between 0.3 and 0.5 of design speed since the maximum efficiency was estimated at 0.4 of design speed (fig. 6). The maximum efficiency decreases with increasing flow blockage. At 0.7 of design speed, the losses in efficiency resulting from blocking 22, 55, and 75 percent of the air flow were approximately 22, 38, and 44 percentage points, respectively. These reductions in efficiency probably result from losses in the eddy flow and in the mixing between the eddy flow and the through flow. For any one flow blockage configuration, the maximum efficiency was nearly constant in the range of 0.4 to 0.7 of design speed.

A comparison of the rotor torque for the three blockage configurations as a percentage of the torque for the unblocked rotor is shown in figure 13. The torque values were referenced to the maximum efficiency points for the unblocked rotor. The ratio of the flow rate at the maximum efficiency point to the flow rate at the maximum flow point for the unblocked rotor was used to determine the torque from each of the torque curves for the various blocked rotor configurations. Since the torque performance curves for both the blocked and unblocked rotor started with the outlet flow control valve in the open position, this method should determine torque values with the outlet flow control valve in approximately the same position (similar downstream resistance). At 0.7 of design speed, blocking 22, 55, and 75 percent of the air flow results in torque values of 83, 64, and 52 percent of the unblocked rotor torque, respectively. At 0.4 of design speed, the corresponding torque values were 108, 73, and 68 percent of the unblocked rotor torque. The proportional reduction in torque is less than the change in flow rate that can be as-

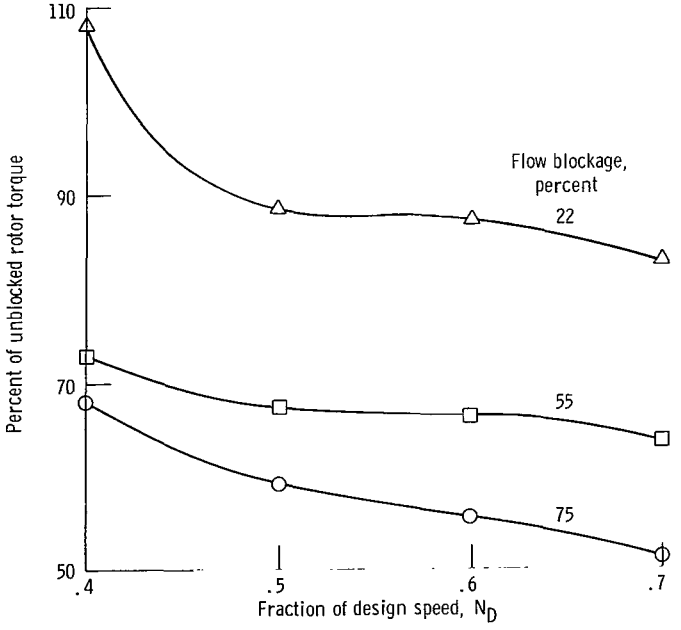

Figure 13. - Comparison of rotor torque for three flow blockage configurations.

sumed to correspond to the blockage area. Apparently, power is absorbed in the eddy flow that circulates ahead of and in the rotor blades in the area where the flow has been blocked. Also indicated is that low flow blockages do not decrease the rotor torque at low speeds.

The torque reductions for blockages of 55 and 75 percent may be large enough to lower the engine starting torque requirements to levels such that a low-cost starting system could be considered for some turbofan-type engines.

At speeds greater than 0.5 of design, substantial reductions in both rotor torque and

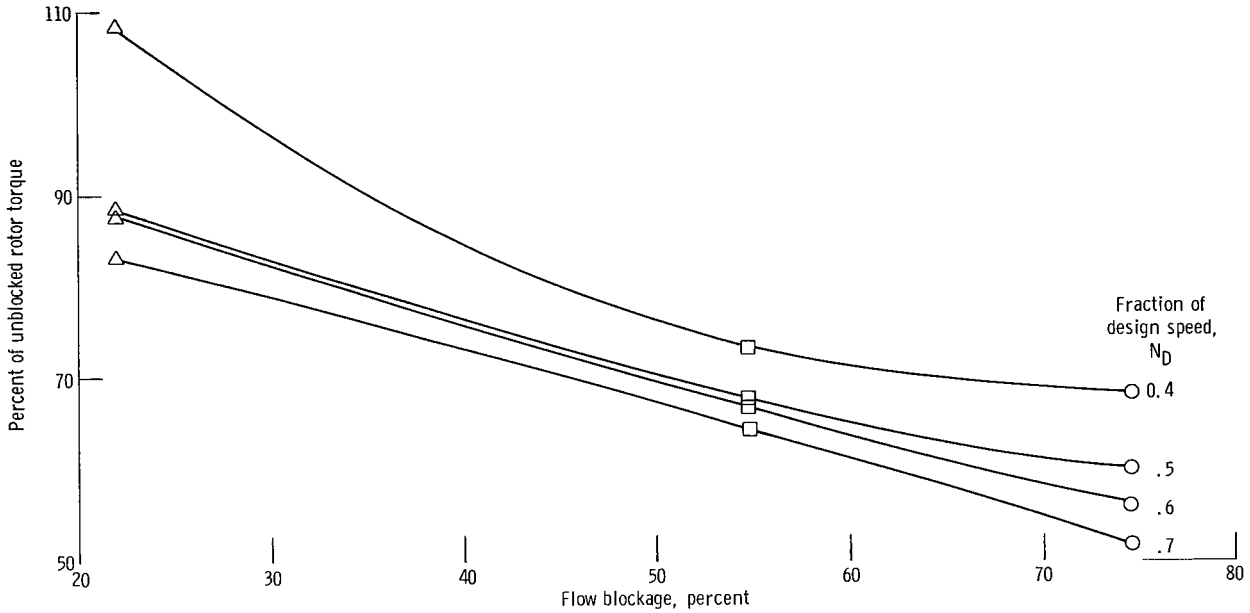

Figure 14. - Rotor torque as function of percent flow blockage for several rotor speeds.

flow rate are indicated for all three blockage configurations. Thus, flow blockage might be useful for reducing engine thrust for aircraft maneuvers where high engine speed and a lowered thrust level are desirable. Flow blockage might also be useful for eliminating rotating stall to enable the engine acceleration characteristics of some engines to be improved.

The rotor torque is shown as a function of flow blockage in figure 14 for rotor speeds between 0.4 and 0.7 of design. Figure 14 is a cross plot of the data presented in figure 13. From figure 14, an estimate of the rotor torque may be obtained for blockages other than those used in this investigation.

SUMMARY OF RESULTS

An inlet-stage axial-flow rotor was tested to speeds as high as 0.7 of design with annulus flow blockages of 22, 55, and 75 percent inserted downstream of the rotor. Such blockage was shown to suppress rotating stall and enable the rotor to be operated under stable conditions to much lower flows than that of the unblocked rotor. In general, the investigation indicated that a flow blockage device might be an effective method of reducing the starting torque requirements of a turbofan engine. In addition, flow blockage might be used for reducing engine thrust for aircraft maneuvers where low thrust and high engine rpm are desirable. Flow blockage might also be of use for improving engine acceleration characteristics of some engines.

The following detailed results were obtained, and where applicable, they are given in order for the 22, 55, and 75 percent flow blockages, respectively.

1. The rotor efficiency was adversely affected by the insertion of the flow blockages, and at 0.7 of design speed, the losses in efficiency were approximately 22, 38, and 44 percentage points.

2. At 0.7 of design speed, the blockages resulted in torque values of 83, 64, and 52 percent of the unblocked rotor torque. At 0.4 of design speed, the corresponding torque values were 108, 73, and 68 percent of the unblocked rotor torque.

3. For the three blockage configurations, the temperature measured just upstream of the blades generally increased from the blade hub to the blade tip and was higher at the hub than in the upstream plenum chamber. The maximum temperature observed was 734° R (408 K) with 55 percent flow blockage. However, for the 75 percent flow blockage, the temperature increased with time, and the equilibrium temperature for this case would probably exceed 734° R (408 K).

4. The blade vibratory stresses were low for all three blockage configurations (3000 psi or 20.65×10^6 N/m^2 maximum). This low stress level indicated an absence of rotating stall that was substantiated by inlet surveys with a hot-wire anemometer probe.

Lewis Research Center,
National Aeronautics and Space Administration,
Cleveland, Ohio, July 28, 1969,
720-03.

REFERENCES

1. Huntley, S. C.:, Huppert, Merle C.; and Calvert, Howard F.: Effect of Inlet-Air Baffles on Rotating-Stall and Stress Characteristics of an Axial-Flow Compressor in a Turbojet Engine. NACA RM E54G09, 1955.

2. Lucas, James G.; Finger, Harold B.; and Filippi, Richard E.: Effect of Inlet-Annulus Area Blockage on Over-All Performance and Stall Characteristics of an Experimental 15-Stage Axial-Flow Compressor. NACA RM E53L28, 1954.

3. Filippi, Richard E.; and Lucas, James G.: Effect of Compressor-Inlet Area Blockage on Performance of an Experimental Compressor and a Hypothetical Engine. NACA RM E54L01, 1955.

4. Chapman, G. E.: Methods of Improving Compressor Off-Design Operation. Presented at the Institute of Aeronautical Sciences Propulsion Meeting, Cleveland, Ohio, Mar. 11, 1955.

5. Glawe, George E.; Krause, Lloyd N.; and Dudzinski, Thomas J.: A Small Combination Sensing Probe for Measurement of Temperature, Pressure, and Flow Direction. NASA TN D-4816, 1968.

NASA-Langley, 1969 —— 28 E-4783

NATIONAL AERONAUTICS AND SPACE ADMINISTRATION
WASHINGTON, D. C. 20546
OFFICIAL BUSINESS

FIRST CLASS MAIL

POSTAGE AND FEES PAID
NATIONAL AERONAUTICS AND
SPACE ADMINISTRATION

POSTMASTER: If Undeliverable (Section 158 Postal Manual) Do Not Return

"The aeronautical and space activities of the United States shall be conducted so as to contribute . . . to the expansion of human knowledge of phenomena in the atmosphere and space. The Administration shall provide for the widest practicable and appropriate dissemination of information concerning its activities and the results thereof."

—NATIONAL AERONAUTICS AND SPACE ACT OF 1958

NASA SCIENTIFIC AND TECHNICAL PUBLICATIONS

TECHNICAL REPORTS: Scientific and technical information considered important, complete, and a lasting contribution to existing knowledge.

TECHNICAL NOTES: Information less broad in scope but nevertheless of importance as a contribution to existing knowledge.

TECHNICAL MEMORANDUMS: Information receiving limited distribution because of preliminary data, security classification, or other reasons.

CONTRACTOR REPORTS: Scientific and technical information generated under a NASA contract or grant and considered an important contribution to existing knowledge.

TECHNICAL TRANSLATIONS: Information published in a foreign language considered to merit NASA distribution in English.

SPECIAL PUBLICATIONS: Information derived from or of value to NASA activities. Publications include conference proceedings, monographs, data compilations, handbooks, sourcebooks, and special bibliographies.

TECHNOLOGY UTILIZATION PUBLICATIONS: Information on technology used by NASA that may be of particular interest in commercial and other non-aerospace applications. Publications include Tech Briefs, Technology Utilization Reports and Notes, and Technology Surveys.

Details on the availability of these publications may be obtained from:

SCIENTIFIC AND TECHNICAL INFORMATION DIVISION

NATIONAL AERONAUTICS AND SPACE ADMINISTRATION

Washington, D.C. 20546